ELSEVIER

Physica D 119 (1998) 73–87

PHYSICA D

1D phonon scattering by discrete breathers

Thierry Cretegny [a,*], Serge Aubry [b], Sergej Flach [c]

[a] *Laboratoire de Physique de l'Ecole Normale Supérieure de Lyon, CNRS URA 1325, 46 allée d'Italie, 69007 Lyon, France*
[b] *Laboratoire Léon Brillouin (CEA – CNRS), CE Saclay 91191-Gif-sur-Yvette Cedex, France*
[c] *Max-Planck-Institut für Physik komplexer Systeme, Bayreuther Str. 40 H.16, D-01187 Dresden, Germany*

Received 11 June 1997; received in revised form 16 October 1997
Communicated by F.H. Busse

Abstract

At the zero amplitude limit, the scattering of 1D phonons by a spatially symmetric exact breather is equivalent to the linear scattering by a time-periodic potential. We first study situations with a single-channel scattering where the breather reemits phonons only at the frequency of the incoming wave ω. In that case, the incoming flux of energy is proven to be identical to the outgoing flux (elastic scattering). An extension of Levinson's theorem is proven and illustrated numerically on examples. The influence of internal modes of the breather on the scattering outcome is analysed.

We next study situations with a multi-channel scattering where phonons are reemitted not only at the frequency of the incoming wave ω but also at another harmonic frequency $\omega + n\omega_b$. For such a scattering, it is proven that the reemitted outgoing flux of energy is necessarily larger than the energy flux of the incoming wave. As a result, the breather radiates energy with a flux proportional to the incoming flux. Its energy decays slowly and linearly over a very long period of time until it reaches another regime. This prediction is confirmed by a numerical simulation. © 1998 Elsevier Science B.V.

1. Introduction

The breathers which are observed in the molecular dynamics of a nonlinear model do not have an infinite lifetime (unless the initial condition is specifically chosen) and thus cannot be the exact breather solutions of the model. Although in a thermalized system they may persist over a long period of time, breathers appear, grow or decay and disappear essentially because of their interactions with their environment. This one can be considered as consisting of a radiation bath (phonons) and other moving or nonmoving breathers.

The first step for studying this interaction is to consider the (linear) scattering of phonons by an exact breather solution in the limit where the amplitude of the phonons goes to zero. A second step will be to consider the corrections to this linear scattering due to the nonlinearity taken at the lowest significant order. Further development of the theory should help, for example, to understand some features observed in breather collisions [1], which

* Corresponding author. Tel.: +33 4 72 72 81 38; fax: +33 4 72 72 80 80; e-mail: tcretegn@physique.ens-lyon.fr.

PII S0167-2789(98)00066-9

lead to breather growth. This paper presents partial results concerning only the linear scattering of phonons on spatially symmetric breathers in 1D Klein–Gordon (KG) chains. Mathematical details and extensions to more general models without symmetry requirements, will be described later in [2]. The Lagrangian of KG chains has the form:

$$\mathcal{L} = \sum_n \frac{1}{2}\dot{u}_n^2 - V(u_n) - \frac{1}{2}C(u_n - u_{n-1})^2. \tag{1}$$

Here $V(x)$ is an on-site anharmonic potential and the coupling between the nearest neighbour particles is harmonic with constant $C > 0$. In this class of models, the existence of breathers has been proven for C not too large [3]. These exact breathers solutions can be calculated using the accurate numerical techniques developed in [4] and improved later in [5].

We choose the following potentials $V(x)$ for our numerical illustrations

$$V(x) = \tfrac{1}{2}x^2 - \tfrac{1}{3}x^3 \quad \text{(cubic)}. \tag{2}$$

$$V(x) = \tfrac{1}{2}(1 - \mathrm{e}^{-x})^2 \quad \text{(Morse)}, \tag{3}$$

which have their stable minimum at $x = 0$ with $V''(0) = 1$. Let us consider a time reversible and spatially symmetric breather $\{u_n(t)\}$ with period $t_\mathrm{b} = 2\pi/\omega_\mathrm{b}$. It fulfills

$$\ddot{u}_n + V'(u_n) - C\Delta_2 u_n = 0 \tag{4}$$

and the conditions $\lim_{n\to\infty} u_n(t) = 0$, $u_n(-t) = u_n(t)$, $u_n(t + t_\mathrm{b}) = u_n(t)$ and $u_{-n}(t) = u_n(t)$. ($\Delta_2 u_n = u_{n+1} - 2u_n + u_{n-1}$ is the standard discrete Laplacian.)

2. Phonon scattering by a time-periodic potential

The transmission coefficient of a phonon [1] through a breather can be calculated directly from a numerical experiment consisting in launching a small amplitude quasi-monochromatic wave packet towards the breather, initially far away, and measuring the amplitude of the wave packet transmitted through this breather. The advantage of this method, which is used in [6], is that it describes the real interaction of the phonon with the breather without truncating any nonlinear terms but it demands careful and long calculations in order to produce accurate results. Moreover, as explained in [6], it is difficult to study the scattering at wave lenghts where the group velocity becomes too small.

A more elegant method which we shall use here, consists in calculating numerically the exact scattering scheme for a given incoming wave and the corresponding outgoing waves. It is obtained as a solution of the linearized equations fulfilled by the small perturbations of the breather (Hill equation)

$$\ddot{\varepsilon}_n + V''(u_n(t))\varepsilon_n - C\Delta_2\varepsilon_n = 0. \tag{5}$$

These calculations are fast and highly accurate. They reproduce quite well the results obtained with the direct measurements provided the incoming wave packet of the latter ones have a sufficiently small amplitude and a well-determined frequency.

[1] Let us stress that in this classical problem, the term "phonon" means linear lattice waves.

Eq. (5) also determines the linear stability of the breather. Since their coefficients are time periodic with period t_b, the linear stability is determined by the properties of the spectrum of the Floquet matrix $\boldsymbol{F}$. Integration of Eq. (5) relates linearly $\varepsilon(t) = \{\varepsilon_n(t)\}$ and $\dot{\varepsilon}(t) = \{\dot{\varepsilon}_n(t)\}$ at time $t = t_b$ to its initial conditions at time $t = 0$:

$$\begin{pmatrix} \varepsilon(t_b) \\ \dot{\varepsilon}(t_b) \end{pmatrix} = \boldsymbol{F} \cdot \begin{pmatrix} \varepsilon(0) \\ \dot{\varepsilon}(0) \end{pmatrix}. \tag{6}$$

This matrix is symplectic which implies that its set of eigenvalues is invariant by conjugacy and inversion (see [7] for details). By definition, a breather is said to be *linearly stable* when all the eigenvalues of its Floquet matrix $\boldsymbol{F}$ lie on the unit circle.[2] This property means that any small perturbation will not grow exponentially in time.[3] An eigenvector of the Floquet matrix $\{\varepsilon_n(0), \dot{\varepsilon}_n(0)\}$ with an eigenvalue $e^{i\theta}$ on the unit circle, corresponds to a solution of Eq. (5) which fulfills a Bloch condition

$$\varepsilon_n(t + t_b) = e^{-i\theta t/t_b}\varepsilon_n(t). \tag{7}$$

For an infinite system with a single breather, the spectrum of the Floquet matrix $e^{i\theta}$ contains an absolutely continuous part which is the spectrum obtained for the system without the breather (with $u_n(t) \equiv 0$). There exists a value of q such that θ fulfills

$$\theta = \pm\omega(q)t_b \pmod{2\pi} = \pm 2\pi \frac{\omega(q)}{\omega_b} \pmod{2\pi}, \tag{8}$$

where $\omega(q)$ is the standard phonon dispersion of the KG chain

$$\omega(q) = \sqrt{1 + 4C \sin^2 q/2}. \tag{9}$$

The associated eigenstates correspond to the scattering scheme of the phonons we are looking for. The spectrum of $\boldsymbol{F}$ may also contain a discrete part corresponding to spatially exponentially localized states. The corresponding modes are called internal modes of the breather (see e.g. [10]).

Because of Eq. (7), $\{\chi_n(t) = e^{-i\theta t/t_b}\varepsilon_n(t)\}$ is time periodic with period t_b. It is convenient to use the Fourier coefficients as new variables

$$\varepsilon_n(t) = \sum_j \alpha_n^j e^{-i(\omega(q)+j\omega_b)t}, \tag{10}$$

$$V''(u_n(t)) = \sum_j \beta_n^j e^{-ij\omega_b t} \tag{11}$$

(if the on-site potential is even, then $\beta_n^j = 0$ for j odd) so that Eq. (5) becomes

$$-C\Delta_2\alpha_n^j + \sum_k \beta_n^{j-k}\alpha_n^k = (\omega(q) + j\omega_b)^2\alpha_n^j. \tag{12}$$

The index j labels the amplitudes of the wave in the channel at frequency $\omega(q) + j\omega_b$. For large $|n|$, β_n^j becomes independent of n and zero for $j \neq 0$, so that the wave propagation in the different channels becomes uncoupled.

[2] For the standard quantum scattering problem by a time-periodic potential [8], described by a linear equation with the form $H(t)\psi(t) = i\dot{\psi}(t)$ (which could be written similarly to Eq. (12)), $\boldsymbol{F}$ is the evolution operator over one period of time and is also unitary. Thus, unlike the case treated here, all its eigenvalues are forced to stay on the unit circle.

[3] Note that linear stability does not imply strict stability. Actually, any linearly stable breather is generally unstable in the strict sense because there exist perturbations which grow linearly in time (for example a perturbation which slightly changes the frequency of the breather (marginal mode [9])).

The amplitude of a wave at a frequency ω which is not in the phonon band, decays exponentially to zero for large $|n|$ as $\exp -|n|/\xi(\omega)$. The characteristic length $\xi(\omega)$ is defined by the equations

$$\sinh^2 \xi(\omega)/2 = \frac{1-\omega^2}{4C} \quad \text{when } |\omega| < 1, \tag{13}$$

$$\cosh^2 \xi(\omega)/2 = \frac{\omega^2-1}{4C} \quad \text{when } \sqrt{1+4C} < |\omega|. \tag{14}$$

In particular, the breather harmonics at $j\omega_b$ are not in the phonon band, and decay exponentially with the characteristic length $\xi(j\omega_b)$. Thus, the global characteristic size of the breather is $\xi_b = \sup_j \xi(j\omega_b)$.[4]

For the channels j, where $\omega_j = \omega(q) + j\omega_b$ is not in the phonon band $\pm\omega(q')$, the wave amplitude α_n^j decays exponentially with a characteristic length shorter than or equal to $\xi_j = \mathrm{Max}(\xi(\omega_j), \xi_b)$. These channels are said to be *inactive* and *active* in the opposite case.

The generic condition, that the harmonics $j\omega_b$ of the breather are not in the phonon band defined by $\pm\omega(q)$, implies that $0 < \omega(\pi) - \omega(0) = \sqrt{1+4C} - 1 < \omega_b$. Thus, if ω_j is in the phonon band for $j \neq 0$, there exists a q' such that $\omega_j = \omega(q) + j\omega_b = -\omega(q')$ and this value of j is unique. In other words the two symmetric arcs corresponding to the absolutely continuous part (8) of the spectrum of the Floquet matrix, overlap on the unit circle.[5] As a result, only one or two channels at most may be active which yields two possible situations:

- A one-channel scattering when for any $j \neq 0$, ω_j is not in the phonon band. Only channel 0 is active and propagates waves at infinity. An incoming wave with frequency $\omega(q)$ and wave vector q will generate propagating outgoing waves at the same frequency $\omega(q)$ and wave vector $\pm q$.
- A two-channel scattering when there exists $j \neq 0$ (unique) such that $\omega_j = \omega(q) + j\omega_b = -\omega(q')$. An incoming wave with frequency $\omega(q)$ and wave vector q, will generate outgoing waves not only at frequency $\omega(q)$ and wave vector $\pm q$, but also at frequency $-\omega(q')$ and wave vector $\pm q'$.

When $|n|$ is large compared to $\xi_a = \sup_j \xi(\omega_j)$ (see footnote 4) for ω_j not in the phonon band, the solution of Eq. (5) becomes a superposition of plane waves in the active channels. Thus, the scattering at frequency $\omega(q)$ can be performed on finite systems provided it is significantly larger than these characteristic lengths which are generally not very large.

An essential property of plane wave scattering is that the total momentum of the phonons is conserved. This property is easily proven:

Let $\{\varepsilon_n(t)\}$ be a solution of the linearized equations (5). Let us multiply both sides of these equations by ε_n^* and take the imaginary part. We obtain

$$C\,\mathrm{Im}(\varepsilon_n^*\varepsilon_{n-1} - \varepsilon_n\varepsilon_{n+1}^*) = \mathrm{Im}\varepsilon_n^*\ddot{\varepsilon}_n = \mathrm{Im}\frac{\mathrm{d}}{\mathrm{d}t}\varepsilon_n^*\dot{\varepsilon}_n. \tag{15}$$

Averaging over time, one gets

$$\langle \mathrm{Im}\,\varepsilon_n^*\varepsilon_{n-1}\rangle = \langle \mathrm{Im}\,\varepsilon_{n+1}^*\varepsilon_n\rangle = -J. \tag{16}$$

The momentum J of the solution $\varepsilon_n(t)$ is independent of n. The momentum of a single plane wave $a\mathrm{e}^{\mathrm{i}(qn-\omega t)}$ is $J = |a|^2 \sin q$. For large $|n|$, $\varepsilon_n(t)$ is just a sum of plane waves in the active channels. One finds readily that J is the sum of the contributions of each wave and has to be the same distance away from the breather at the right side and the left side.

[4] When the on-site potential is even, the breather harmonics are odd so that ξ_b and ξ_a are defined as a supremum over j for j odd only.

[5] In that situation, the breather may be linearly unstable for finite size systems but recovers its linear stability for the infinite system as shown in [10].

3. One-channel scattering

For one-channel scattering, the incoming and outgoing phonons have the same frequency $\omega(q)$.

3.1. The scattering matrix

For large $|n| \gg \xi_a$, on both sides of the breather, the solution of Eq. (5) is the sum of two plane waves running in opposite directions:

$$\begin{aligned} \varepsilon_n &= a_+ e^{iqn - i\omega(q)t} + b_- e^{-iqn - i\omega(q)t} \quad \text{for } n \ll -\xi_a, \\ \varepsilon_n &= b_+ e^{iqn - i\omega(q)t} + a_- e^{-iqn - i\omega(q)t} \quad \text{for } n \gg \xi_a. \end{aligned} \tag{17}$$

Eq. (5) implies a linear relation between the amplitudes of the incoming waves and the outgoing waves with the *scattering matrix*:

$$\begin{pmatrix} b_+ \\ b_- \end{pmatrix} = \boldsymbol{M}(q) \begin{pmatrix} a_+ \\ a_- \end{pmatrix}, \quad \text{with } \boldsymbol{M}(q) = \begin{pmatrix} M_{++} & M_{+-} \\ M_{-+} & M_{--} \end{pmatrix}. \tag{18}$$

The momentum conservation relation, Eq. (16), yields $|a_+|^2 - |b_-|^2 = |b_+|^2 - |a_-|^2$, which implies that $\boldsymbol{M}$ is unitary. In this paper, we restrict our study to space symmetric breathers ([2] for the general case). Since $\varepsilon_{-n}(t)$ is also a solution of Eq. (5), we find $M_{++} = M_{--}$ and $M_{+-} = M_{-+}$. With this condition, the unitary matrix $\boldsymbol{M}(q)$ can be written as

$$\boldsymbol{M}(q) = e^{i\gamma(q)} \begin{pmatrix} i\sin\alpha(q) & \cos\alpha(q) \\ \cos\alpha(q) & i\sin\alpha(q) \end{pmatrix}, \tag{19}$$

where $\alpha(q)$ and $\gamma(q)$ are parameters. The eigenvectors of $\boldsymbol{M}(q)$ are $(1\ \ 1)^t$ for the eigenvalue $\lambda_+ = e^{i(\gamma+\alpha)}$ and $(-1\ \ 1)^t$ for the eigenvalue $\lambda_- = e^{i(\gamma-\alpha)}$.

The corresponding scattering schemes are, respectively:

$$\begin{aligned} \varepsilon_{n\pm}(t) &= \pm\cos(qn - \delta_\pm/2)e^{-i\omega(q)t}, \quad n \ll -\xi_a, \\ \varepsilon_{n\pm}(t) &= \cos(qn + \delta_\pm/2)e^{-i\omega(q)t}, \quad n \gg \xi_a, \end{aligned} \tag{20}$$

where we introduced the phase shifts for the spatially symmetric and antisymmetric states: $\delta_+(q) = \gamma + \alpha$ and $\delta_-(q) = \gamma - \alpha$.

The scattering scheme with only one incoming wave say from the left is obtained for $a_+ = 1$ and $a_- = 0$. Then we find that the transmission coefficient is

$$T(q) = |M_{++}(q)|^2 = |M_{--}(q)|^2 = \sin^2\alpha(q) = \sin^2\frac{\delta_+(q) - \delta_-(q)}{2}. \tag{21}$$

3.2. Scattering at the band edge

With the convention that the signs of q and $\omega(q)$ are the same, the complex conjugate of Eq. (17) gives a scattering scheme for $-q$ for which the amplitude of the waves a_+,a_-, b_+,b_- are changed by their complex conjugate. This yields $\boldsymbol{M}(-q) = \boldsymbol{M}^*(q)$.

We assume here that the scattering matrix $\boldsymbol{M}(q)$ is a continuous function of q, which implies at the band edge that $\boldsymbol{M}(0)$ and $\boldsymbol{M}(\pi)$ become real matrices. Let us consider the case $q = 0$ to fix the ideas. We have

either $\alpha(0) = 0 \bmod \pi$ and $\gamma(0) = 0 \bmod \pi$ or $\alpha(0) = \pi/2 \bmod \pi$ and $\gamma(0) = \pi/2 \bmod \pi$. These conditions imply:

$$\boldsymbol{M}(0) = \pm\boldsymbol{\sigma} \quad \text{or} \quad \boldsymbol{M}(0) = \pm\mathbf{1}, \tag{22}$$

with

$$\boldsymbol{\sigma} = \begin{pmatrix} 0 & 1 \\ 1 & 0 \end{pmatrix} \quad \text{and} \quad \mathbf{1} = \begin{pmatrix} 1 & 0 \\ 0 & 1 \end{pmatrix}. \tag{23}$$

(1) When, $\boldsymbol{M}(0) = \pm\boldsymbol{\sigma}$, the transmission coefficient $T(0)$ vanishes at the band edge.
When $\boldsymbol{M}(0) = -\boldsymbol{\sigma}$, it follows from Eq. (20) that $\varepsilon_n(t) \equiv 0$, which means that there is no bounded solution at $q = 0$ for Eq. (5). This is the generic case which is found numerically at the band edge.
When $\boldsymbol{M}(0) = \boldsymbol{\sigma}$, Eq. (20) implies that there are two independent bounded solutions at $q = 0$ for Eq. (5). Although we can construct rather artificially examples of such a situation with static potentials, we did not find (yet?) realistic examples with breathers where this situation occurs.

(2) When, $\boldsymbol{M}(0) = \pm\mathbf{1}$, the transmission coefficient $T(0)$ is unity at the band edge.
Eq. (20) yields only one independent solution $\varepsilon_n(t) = 1$ for $n \gg \xi_a$ and $\varepsilon_n(t) = \pm 1$ for $n \ll -\xi_a$. It is spatially symmetric for $\boldsymbol{M}(0) = \mathbf{1}$ and spatially antisymmetric for $\boldsymbol{M}(0) = -\mathbf{1}$. Our numerical results suggest that such an extended state exists at the band edge as a limit of a localized state that is when an internal mode of the breather is just appearing before it detaches from the band.

This result is in agreement with the result of Kim et al. [11] which states that the transmission coefficient at the band edge is one at a localization threshold when a localized state just appears and is zero otherwise. However, let us emphasize now that this property is a consequence of the spatial symmetry of the breather. Our extended theory [2] predicts that when this symmetry is broken, $T(0)$ is still zero provided there are no states at the band edge but $T(0)$ is no more necessarily 1 at a localization threshold. The same results hold at the other edge of the band for $q = \pi$.

3.3. Levinson's theorem

For a finite system, the continuous spectrum of $\boldsymbol{F}$ is reduced to a discrete set of eigenvalues. Considering a system with size $2N$ (with $N \gg \sup_q \xi_a(q)$) and the periodic boundary condition $\varepsilon_{n+2N}(t) = \varepsilon_n(t)$, the eigenvalues and eigenvectors are obtained very accurately from those of the infinite system [6] by imposing that boundary condition on Eq. (20). We find that only a discrete subset of the continuous set of wave vectors q, $\{q_{p+}\}$ and $\{q_{p-}\}$ is selected:

$$2Nq_{p+} + \delta_+(q_{p+}) = 2p\pi \quad \text{(spatially symmetric states)}, \tag{24}$$

$$2Nq_{p-} + \delta_-(q_{p-}) = \pi + 2p\pi \quad \text{(spatially antisymmetric states)}, \tag{25}$$

where p is some integer.

For this system, $\boldsymbol{F}$ has $N + 1$ symmetric eigenmodes and $N - 1$ antisymmetric eigenmodes. Formulas (24) and (25) allow to count the number of symmetric and antisymmetric states in the band, which yields by difference the number of states strictly outside of the band. [7]

[6] The error is bounded from above by e^{-N/ξ_a}.

[7] These missing eigenvalues might be either on the unit circle outside the band, or outside the unit circle (then implying the breather instability), but in any case correspond to spatially exponentially localized modes.

Denoting the number of these localized modes of the Floquet operator for each symmetry $\pm$ by $N_{b\pm}$, it follows

$$N_{b+} = -\mathrm{Int}\left(-\frac{\delta_+(0)}{2\pi}\right) - \mathrm{Int}\left(\frac{\delta_+(\pi)}{2\pi}\right) \tag{26}$$

and

$$N_{b-} = \mathrm{Int}\left(\frac{\delta_-(0)+\pi}{2\pi}\right) + \mathrm{Int}\left(-\frac{\delta_-(\pi)+\pi}{2\pi}\right). \tag{27}$$

(Note that the function $\mathrm{Int}(x)$ is defined as the largest integer smaller than or equal to x.)

4. Numerical calculation of one-channel scattering

4.1. Numerical technique

The time reversible solutions of Eq. (5) fulfilling condition (7) are calculated for a finite system for $n = -N \cdots N$ with forced boundary conditions: $\varepsilon_{N+1}(t) = \mathrm{e}^{-\mathrm{i}\omega(q)t}$ and $\varepsilon_{-N-1}(t) = \varepsilon_{N+1}(t)$ for the spatially symmetric states or $\varepsilon_{-N-1}(t) = -\varepsilon_{N+1}(t)$ for the spatially antisymmetric states. N has to be large enough compared to $\xi_a(q)$ in order for the solution to be a superposition of plane waves close to the boundaries of the system. In practice, $\xi_a(q)$ is generally not very large, and a relatively small system size is sufficient. We also take advantage of the spatial symmetry of the breather by fixing $\varepsilon_n(t) = \pm\varepsilon_{-n}(t)$. Thus we obtain solutions which are independent of the size and correspond to those of the infinite system.

Integration of Eq. (5) with an additional one corresponding to the forced boundary conditions determines the following operator:

$$\boldsymbol{G}(\varepsilon(0), \dot{\varepsilon}(0)) = \begin{pmatrix} \varepsilon(0) \\ \dot{\varepsilon}(0) \end{pmatrix} - \mathrm{e}^{\mathrm{i}\omega(q)t_\mathrm{b}} \begin{pmatrix} \varepsilon(t_\mathrm{b}) \\ \dot{\varepsilon}(t_\mathrm{b}) \end{pmatrix}. \tag{28}$$

The solutions fulfilling (7) are zeroes of this operator which can be calculated in one step from any trial initial solution with a Newton method. Close to both boundaries the spatially symmetric and antisymmetric solutions are found to be plane wave superpositions with wave vectors $+q$ and $-q$. Their amplitudes determine the phase shift $\delta_+(q)$ or $\delta_-(q)$ from which the transmission coefficient $T(q)$ is deduced at the computer accuracy using formula (21).

4.2. Illustration of the extended Levinson theorem

Let us now present some numerical applications. First, we consider a linearly stable breather at frequency $\omega_\mathrm{b} = 0.85$ with the cubic on-site potential (2). The variation of the arguments θ of the eigenvalues $\mathrm{e}^{\mathrm{i}\theta}$ of its Floquet matrix $\boldsymbol{F}$ in the interval $[0, \pi]$ is shown versus the coupling C in Fig. 1. The magnification of the bottom of the phonon band shows that a spatially symmetric mode escapes from the band at $C \approx 0.05$ and a spatially antisymmetric mode at $C \approx 0.11$. The phase shifts and the transmission coefficients versus the phonon wave vector q are shown in Fig. 2 below the localization threshold of the symmetric state (at $C = 0.04$), at the threshold ($C \approx 0.05$), between the first and second thresholds at $C = 0.08$ and beyond the localization threshold of the spatially antisymmetric state ($C = 0.15$).

One finds easily from Fig. 2 that the predictions of the above extended Levinson theorem are fulfilled: we find precisely $\delta_+(0) = 0$ at the first localization threshold at $C = 0.05$. Fig. 2(d) shows that the phonon

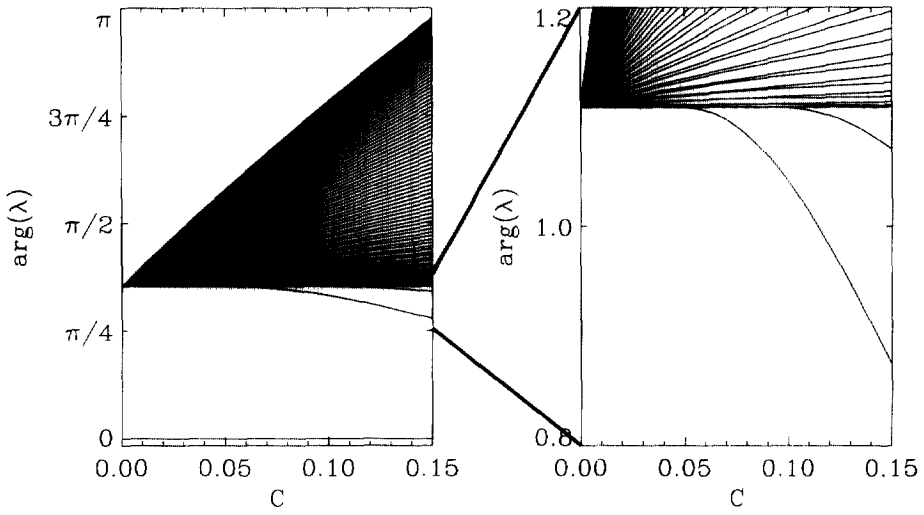

Fig. 1. (a) Arguments of the Floquet eigenvalues of a breather of frequency $\omega_b = 0.85$ (cubic on-site potential (2)) versus the coupling intensity C. (b) Magnification of (a).

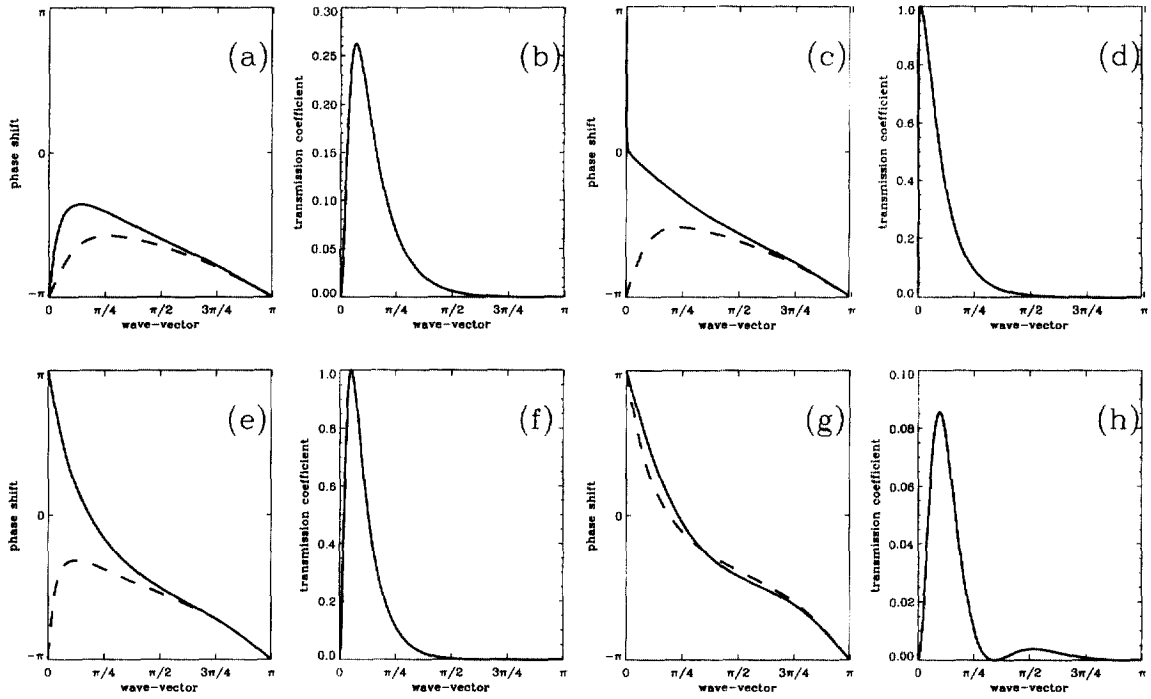

Fig. 2. (a), (b) Phase shifts δ_+ (full line) and δ_- (dashed line) and transmission coefficient of phonons through a "cubic" breather at frequency $\omega_b = 0.85$ and coupling intensity $C = 0.04$ versus q; (c), (d) the same for $C \approx 0.05$; (e), (f) the same for $C = 0.08$; (g), (h) the same for $C = 0.15$.

transmission becomes total at $q = 0$, in contrast to $C = 0.04$, where it vanishes. For larger C, there is a wave vector at $q \neq 0$ where the phonon transmission is total (cf. Fig. 2(f)), as long as $\delta_+(0) \neq \delta_-(0)$. Beyond the localization threshold of the antisymmetric mode at $C \approx 0.11$, the phonon transmission becomes partial for any q.

When C is increased further, $\delta_+(q)$ approaches $\delta_-(q)$ in the whole phonon band, which causes the transmission coefficient to become small again for each value of q. In addition, since curves $\delta_+(q)$ and $\delta_-(q)$ intersect, the phonon transmission totally vanishes at some wave vector.

These results confirm that each appearance (or disappearance) of an internal mode is associated with a sharp change in the phonon transmission. A more general proof of the extended Levinson's theorem applicable to one-channel scattering through discrete nonspatially symmetric breathers in 1D models with nonnearest neighbour coupling will be given in [2].

4.3. *The filtering breather*

In some cases, an internal mode of the breather seems to "enter" the phonon band with an opposite Krein signature [7]. Fig. 3 shows the variation of the arguments of the Floquet eigenvalues of a breather with the Morse on-site potential (3) versus the coupling C. There are two localized states (one spatially symmetric and one spatially antisymmetric) which escape from one phonon band and apparently cross the other phonon band. According to our extended Levinson's theorem (26), the total variation of the phase shifts $\delta_+(0) - \delta_+(\pi)$ should be reduced by 2π when the spatially symmetric mode enters the phonon band. The same holds for the spatially antisymmetric mode. Actually, what is numerically observed (see Fig. 4(a)) is the opposite! A careful analysis [10] of the real behaviour of the Floquet eigenvalue associated with the localized mode shows that it does not cross the band but that just after it collides with the band, a pair of eigenvalues gets out of the unit circle (one inside and one outside because $\boldsymbol{F}$ is symplectic) and moves away from but close to the phonon band. Thus, we must have one

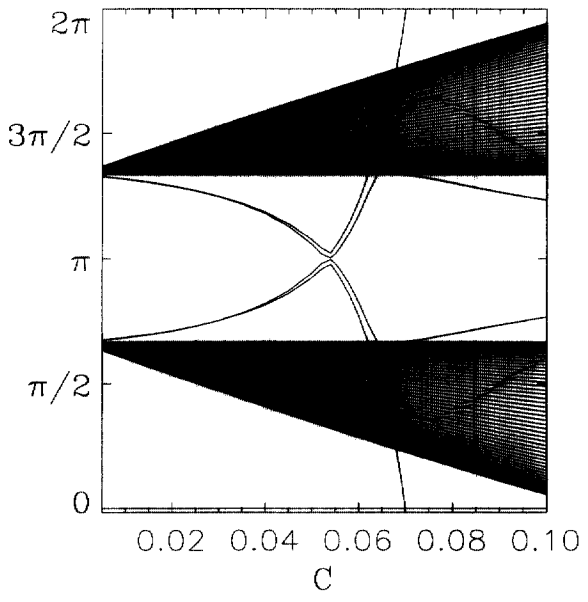

Fig. 3. Argument of the Floquet eigenvalues of a breather at frequency $\omega_b = 0.6$ (Morse potential (3) versus coupling C.

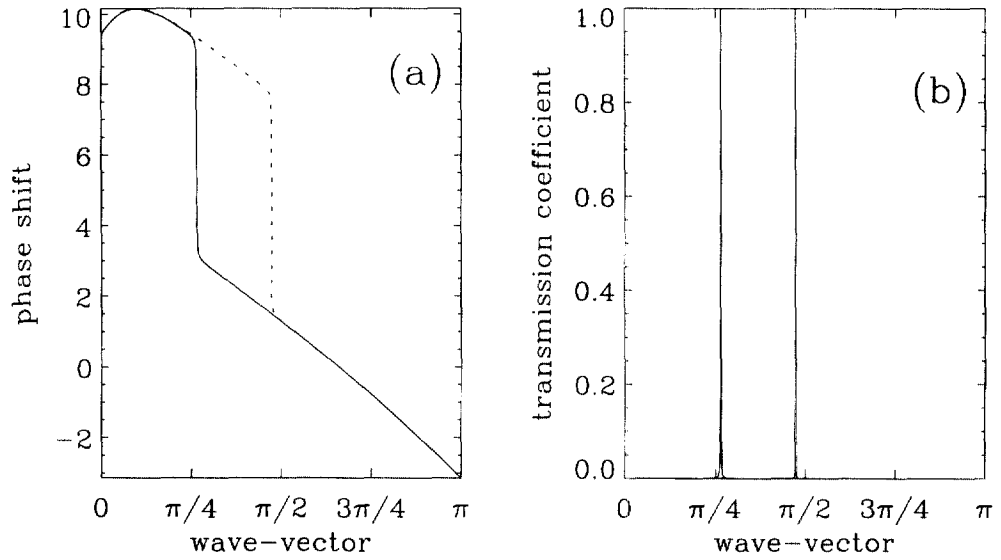

Fig. 4. (a) Phase shifts $\delta_+(q)$ (full line) and $\delta_-(q)$ (dashed line) versus q at $\omega_b = 0.6$ and $C = 0.065$ for the Morse potential (3). (b) Corresponding transmission coefficient versus q.

extra eigenvalue leaving the band, and consequently $\delta_+(0) - \delta_+(\pi)$ must increase by 2π when the localized eigenmode collides with the band as we do observe. Counting the number of localized spatially symmetric modes on Fig. 4(a) with formula (26) yields that three symmetric modes are out of the band: they correspond to the phase mode (i.e. the perturbation which is tangent to the trajectory in the phase space) with eigenvalue 1 ($\theta = 0$) and the above mentioned pair of modes. Counting the number of antisymmetric modes with formula (27) yields two modes which correspond to another pair of eigenvalues outside the unit circle again in agreement with our prediction.

The existence of a pair of eigenvalues of the Floquet matrix close to the phonon band produces a sharp decrease of the phase shift $\delta_+(q)$ by 2π when $e^{i\theta(q)}$ is close to this pair of unstable eigenvalues. (Our high numerical accuracy ensures that it cannot be a true discontinuity.) The same effect is found for the antisymmetric mode on the sharp variation observed for $\delta_-(q)$ (cf. Fig. 4(a)).

In our example, the variation of $\delta_+(q)$ and $\delta_-(q)$ is very sharp which means that the pairs of eigenvalues remain very close to the unit circle. As a result, the breather instability is so weak that it is not observed during the time scale of our numerical experiments.

The transmission coefficient (Fig. 4(b)) calculated from formula (21), is almost zero for most values of q except at two wave vectors q_S and q_{AS}, where there is a very sharp peak which reaches unity with a total transmission. This situation occurs when $e^{i2\pi\omega(q)/\omega_b}$ is very close to one of the two pairs of eigenvalues which are located away from the unit circle.

A direct experiment can check the prediction, that the breather is transparent at two frequencies and opaque elsewhere. We take an initial condition consisting in the superposition of this breather at the centre of the lattice and a gaussian noise at the left with a small amplitude (10^{-2}). (Its spatial Fourier transform is shown in Fig. 5(c).) After a long enough evolution of the fully nonlinear equations of motion, the energy density at the right part of the lattice is shown (Fig. 5(b)). The spatial Fourier transform of the displacements of the transmitted part (cf. Fig. 5(d)) essentially exhibits two narrow peaks at the resonant wave vectors q_S and q_{AS}, which is a nice confirmation of the filtering properties of this breather.

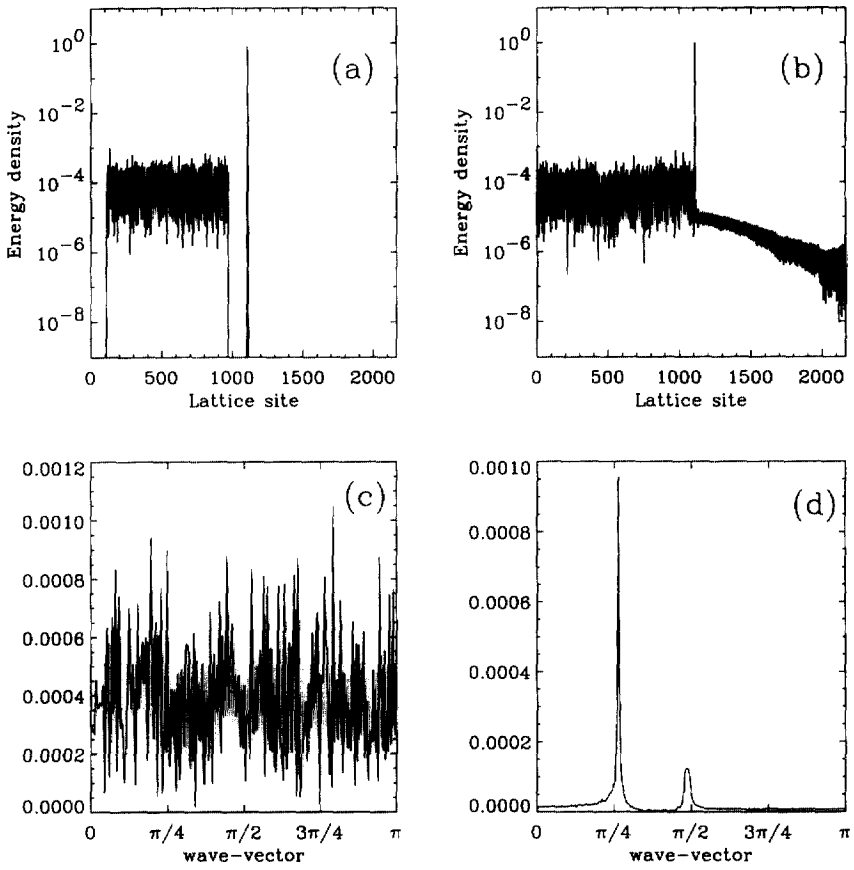

Fig. 5. Scattering of a random perturbation by the breather of Fig. 4: (a), (b) initial and final energy densities in the lattice; (c), (d) spatial Fourier transform of the displacement at the left (resp. right) side of the breather at initial (resp. final) time.

5. Two-channel phonon scattering

When the phonon bands overlap on the unit circle, for $\omega_1 = \omega(q_1) > 0$ ($q_1 > 0$) in the overlap interval, there exist wave vectors $q_2 < 0$ such that $\omega_2 = \omega(q_2) = \omega(q_1) + j\omega_b < 0$ for j integer. In that case, a single incoming wave at frequency ω_1 generates outgoing waves not only at frequency ω_1 but also at ω_2.

The real (or the imaginary) part $\phi_n(t) = \mathrm{Re}\,\varepsilon_n(t)$ is a solution of Eq. (5) which carries an energy flux (per unit of time) $\frac{1}{2}C\langle\phi_n(t)\dot{\phi}_{n+1}(t)\rangle$ from site n to $n+1$ (it is the average power of the force of the atom n acting on the atom $n+1$). The energy flux, carried by a single plane wave $a\cos(qn - \omega t)$ is $\frac{1}{2}C|a|^2\omega\sin q = \frac{1}{2}C\omega J$ and is proportional to its momentum multiplied by the frequency ω. Thus for a single-channel scattering where the incoming and outgoing waves have same frequency, the momentum conservation is equivalent to the energy flux conservation. In that case, the scattering process is *elastic* which means that the incoming flux of energy is identical to the outgoing flux. This is no longer true for a multichannel scattering.

Considering an incoming wave carrying energy towards the breather and outgoing waves carrying energy away of the breather, the asymptotic form of this state is (note that ω_2 and q_2 are negative)

$$\begin{aligned} \varepsilon_n &= \mathrm{e}^{\mathrm{i}q_1 n - \mathrm{i}\omega_1 t} + r_1\mathrm{e}^{-\mathrm{i}q_1 n - \mathrm{i}\omega_1 t} + r_2\mathrm{e}^{-\mathrm{i}q_2 n - \mathrm{i}\omega_2 t}, \quad n \ll -\xi_a, \\ \varepsilon_n &= t_1\mathrm{e}^{\mathrm{i}q_1 n - \mathrm{i}\omega_1 t} + t_2\mathrm{e}^{\mathrm{i}q_2 n - \mathrm{i}\omega_2 t}, \quad n \gg \xi_a. \end{aligned} \tag{29}$$

The momentum conservation equation (16) yields

$$\sin q_1(1-|r_1|^2)-\sin q_2|r_2|^2=\sin q_1|t_1|^2+\sin q_2|t_2|^2 \quad . \tag{30}$$

The energy flux carried by the real (or the imaginary) part of (29), is the sum of the plane waves contributions.[8] It can be decomposed into the sum of an incoming, a reflected and a transmitted flux of energy I,R,T:

$$I=\tfrac{1}{2}C\omega_1\sin q_1, \tag{31}$$

$$R=\tfrac{1}{2}C(\omega_1\sin q_1|r_1|^2+\omega_2\sin q_2|r_2|^2), \tag{32}$$

$$T=\tfrac{1}{2}C(\omega_1\sin q_1|t_1|^2+\omega_2\sin q_2|t_2|^2). \tag{33}$$

Using Eq. (30), the difference between the outgoing flux and the incoming flux of energy

$$R+T-I=\tfrac{1}{2}C(\omega_1-\omega_2)\sin(-q_2)(|r_2|^2+|t_2|^2)>0 \tag{34}$$

is necessarily positive. Consequently, the scattering process is *inelastic*.

This result is illustrated by a calculation of the transmission coefficient through a single breather with band overlap. The numerical technique is the same as presented in Section 4.1 except that in the case of a two-channel scattering, we have to calculate four solutions of Eq. (5) obtained with the four boundary conditions $\varepsilon_{N+1}=e^{i\omega_1 t}$, $\varepsilon_{N+1}=e^{i\omega_2 t}$, and $\varepsilon_{-N-1}(t)=\pm\varepsilon_{N+1}(t)$. Linear combinations of these four solutions yield the scattering solution fulfilling (29) from which we derive $I(q_1)$, $R(q_1)$ and $T(q_1)$.

These results have been obtained considering the incoming phonon as being scattered by a *fixed* time-periodic potential $V''(u_n(t))$. Then, the energy flux which is radiated per unit of time equation (34) is produced by the time dependence of potential. In the real case, the incoming phonon is scattered by the breather and the outgoing energy flux is taken at the expense of the internal breather energy. Then, the breather energy should decay slowly in time with a linear rate given by (34). When the amplitude of the incoming phonon is small, the energy loss of the breather found in a direct simulation is negligible during the numerical experiment and the expected results for the transmitted and reflected energy flux are recovered (see Fig. 6(a)). It can be also checked (Fig. 6(b)) that in addition to the wave vector q_1, wave vector q_2 is also present in the transmitted wave.

When the amplitude of the incoming phonon is not too small, the rate of radiation of the breather becomes large enough to be observable. Then, the breather frequency changes in order to accommodate its loss of energy. For example for a soft potential (e.g. the Morse potential), its frequency ω_b will increase slowly. This situation will last untill either the two-channel scattering ends or the breather becomes linearly unstable. Then another scenario will continue the breather evolution.

The example shown in Fig. 7 concerns a single breather of the KG chain with a Morse potential for which a two-channel scattering is expected. It is "shined" with an appropriate monochromatic phonon with wave vector q_1 at the left side. Then, its frequency increases (while the breather remains located at the same site) , until it reaches an instability threshold. In our example, the unstable mode is a pinning mode (see [9,12,13]). Then, continuing the experiment, the marginal component [9] of this pinning mode turns out to be excited by the incoming wave and the breather starts to move, "surfing" on the incoming wave. It accelerates till it reaches a limit velocity.

[8] This is not true for the special case $\omega_2=-\omega_1$ (and $q_1=-q_2$) which has to be treated separately.

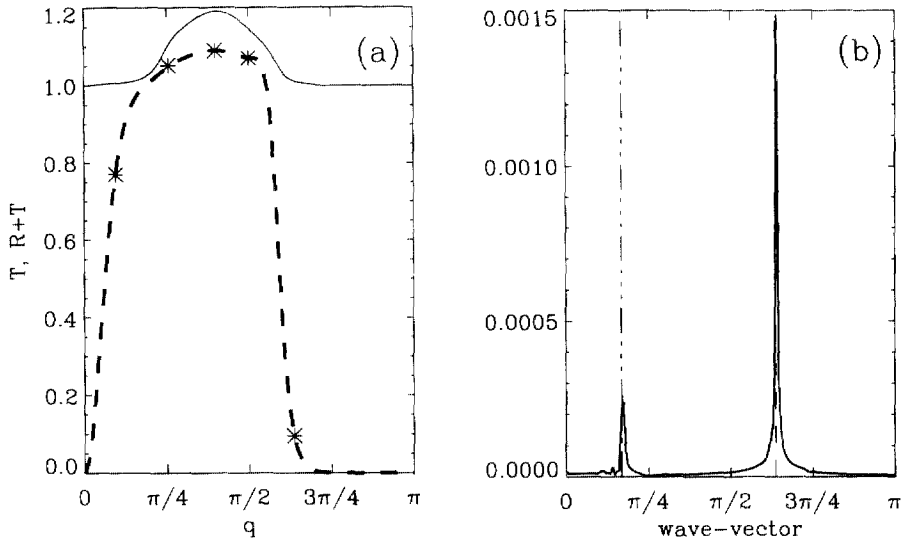

Fig. 6. (a) Transmission coefficient of the energy flux $T(q_1)$ (dashed line) and total outgoing fluxes of energy $T(q_1) + R(q_1)$ (full line) versus q_1 through a single breather for KG chain with the Morse potential (3) at $C = 0.3$ and $\omega_b = 0.8$. The stars correspond to results obtained from a direct simulation of the nonlinear equations of motion. (b) Spatial Fourier transform of the transmitted wave in the direct simulation at $q_1 = 2$.

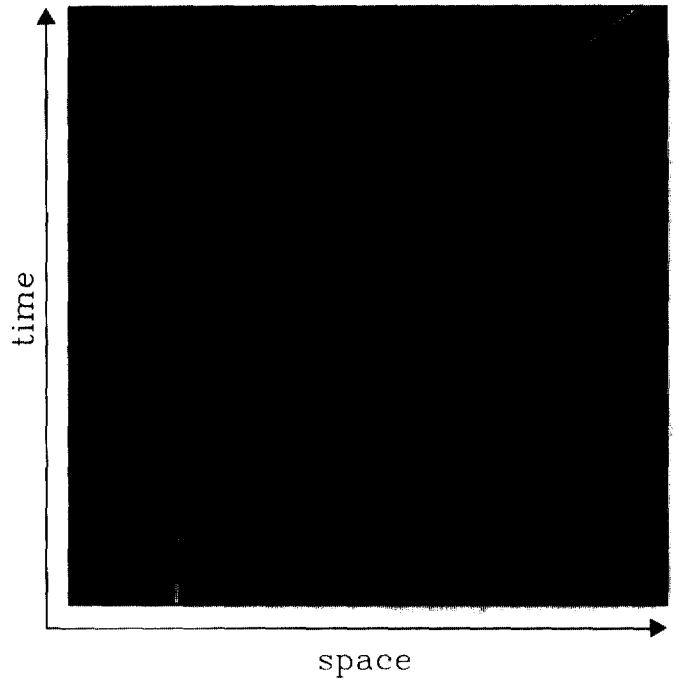

Fig. 7. Energy density in space–time representation for a two-channel inelastic scattering process on a breather. Parameters are $C = 0.2$ and $\omega_b = 0.7$ for the Morse KG chain (3), the wave vector of the incoming wave is $q = 0.8$ and its amplitude is $2 \cdot 10^{-2}$. The breather location (high energy density) versus time appears as the white line. The breather starts to move at the instability threshold when $\omega_b = 0.73$ [13].

6. Conclusion

The linear scattering of phonons by breathers reveals a wide variety of behaviour. Breathers may be almost opaque and essentially reflecting. Then, they behave like static defects for phonons. This could have important physical consequences concerning the energy transport in such nonlinear systems. For example, it has been found in numerical experiments of thermal relaxation in anharmonic systems that energy can be trapped for a very long time, not only by the breathers themselves, but also in some cases, between breathers which are almost opaque to phonons [14].

Breathers may also be totally transparent at some frequencies and there may exist very sharp variations in the transmission coefficient. Actually, full reflection and full transmission are also known in quantum scattering [15].

The role of the internal modes in the breather transparency properties, expected in [11], is explicited by the extended Levinson theorem for time-periodic potentials stated here for the one-channel case. It can be extended to one-channel scattering in a larger class of 1D models without symmetry restrictions [2]. Extension for multi-channel cases as in [8] are also currently studied.

Situations exist where the scattering of phonons involves two channels. Then, it has been proved in that paper that it is necessarily inelastic, that is the breather radiates energy.

Let us end this paper by an anticipation of further works which will demonstrate that any scattering process is inelastic provided the nonlinear expansion be continued far enough. Actually, Eq. (5), which is obtained by linearization of Eq. (4) around a time-periodic breather solution, can be expanded to higher order. Thus, any solution of the linear equations (5) with amplitude a, can be formally continued at some given order p (Birkhoff expansion) to be a solution of the original nonlinear equation at order a^p. For an initial wave at frequency $\omega(q)$, a standard recursive expansion at this order p generates harmonics at frequencies $m\omega(q)+n\omega_b$, where $|m| \leq p$ and n is arbitrary. For p large enough, there are always channels at frequency $p\omega(q)+n\omega_b$ (with n integers) which return into the phonon band. Such channels will be radiating as well as in the two-channel scattering scheme described here. Considering the smallest value of $|p|$ for which this situation occurs, p_0, the scattering process on the breather will necessarily become inelastic and the breather has to loose or gain energy with a rate proportional to I^{p_0}, where I is the incoming flux of energy. This is what we should precisely observe in numerical experiments. As a result any breather which is linearly stable (that is not exponentially unstable), is nevertheless unstable in a strict sense but the rate of instability is only a power of the perturbation and not an exponential.[9] The two-channel scattering process found here, is just the simplest case where this inelastic effect can be exhibited at the lowest order 1.

Acknowledgements

T. Cretegny acknowledges "la Région Rhône-Alpes" for the grant "Emergence".

References

[1] O. Bang, M. Peyrard, Phys. Rev. B 53 (1996) 4143.
[2] T. Cretegny, S. Aubry, S. Flach, K. Kladko, in preparation.
[3] R.S. MacKay, S. Aubry, Nonlinearity 7 (1994) 1623–1643.
[4] J.L. Marín, S. Aubry, Nonlinearity 9 (1996) 1501–1528.
[5] T. Cretegny, S. Aubry, Phys. Rev. B 55 (1997) R11929.
[6] S. Flach, C.R. Willis, in: M. Peyrard (Ed.), Nonlinear Excitations in Biomolecules Springer, Berlin, 1995.

[9] This remark is a *physical* interpretation of the well-known fact that such a Birkhoff expansion yields generally a divergent series.

[7] S. Aubry, Physica D 103 (1997) 201–250.
[8] Ph. Martin, M. Sassoli de Bianchi, Europhys. Lett. 34 (1996) 639.
[9] S. Aubry, T. Cretegny, Physica D 119 (1998) 34–46.
[10] J.L. Marín, S. Aubry, Physica D 119 (1998) 163–174.
[11] S. Kim, C. Baesens, R. MacKay Phys. Rev. E 56 (5) (1997) R4955.
[12] D. Chen, S. Aubry, G. Tsironis, Phys. Rev. Lett. 77 (1996) 4776.
[13] T. Cretegny, J.L. Marín, S. Aubry, in preparation.
[14] G. Tsironis, S. Aubry, Phys. Rev. Lett. 77 (1996) 5225.
[15] A.K. Kazanskii, V.N. Ostrovskii, E.A. Solov'ev, Sov. Phys. JETP 43 (1976) 254.